ACTA IMEKO
ISSN: 2221-870X
December 2024, Volume 13, Number 4, 1 - 9

Dynamic simulation of a novel double Trombe wall to evaluate energy performance in the heating season

Antonio Cristaudo[1], Vittorio Ferraro[2], Francesco Nicoletti[1], Giulia Palermo[1], Dimitrios Kaliakatsos[1]

[1] *Mechanical, Energy and Management Engineering Department, University of Calabria, Via P. Bucci, 87036 Rende (CS), Italy*
[2] *Department of Computer Engineering, Modeling, Electronics, and Systems Engineering, University of Calabria, Via P. Bucci, 87036 Rende (CS), Italy*

ABSTRACT
In the residential building sector, a sustainable human-environment relationship can be achieved by encouraging both the use of renewable sources and the enhancement of energy efficiency in technical systems and building envelopes. This article performs an energy analysis to evaluate the reduction in energy demand attained by installing two Trombe walls on the south-facing wall of the variable orientation test station at the University of Calabria. The two passive systems were symmetrically placed on either side of the existing window system. The assessment of monthly energy demand during the heating season was conducted using the dynamic simulation software DesignBuilder®. To determine the optimal configuration of the Trombe walls, the influence on energy demand related to the materials used for the support structure, the type and number of glasses forming the solar space, the size of the solar space, and the dimensions of the vents were evaluated. The findings indicate that the installation of the two Trombe walls, each comprising two vents with an area of 0.1 m² and a solar space depth of 0.20 m, vertically enclosed by three glass walls with double low-emissivity glazing, results in a 60.62 % reduction in winter energy demand.

Section: RESEARCH PAPER

Keywords: Trombe walls; energy efficiency; passive heating; building optimization

Citation: A. Cristaudo, V. Ferraro, F. Nicoletti, G. Palermo, D. Kaliakatsos, Dynamic simulation of a novel double trombe wall to evaluate energy performance in the heating season, Acta IMEKO, vol. 13 (2024) no. 4, pp. 1-9. DOI: 10.21014/actaimeko.v13i4.1910

Section Editor: Francesco Lamonaca, University of Calabria, Italy

Received July 12, 2024; **In final form** November 19, 2024; **Published** December 2024

Funding: This work was supported by Italian PNRR, Mission 4, Component 2, Investment 1.5, project Tech4You "Technologies for climate change adaptation and quality of life improvement", n. ECS0000009, CUP H23C22000370006.

Corresponding author: Antonio Cristaudo, e-mail: antonio.cristaudo@unical.it

1. INTRODUCTION

The European Commission has embraced the necessity to intervene in mitigating climate change effects through the Green Deal, with the goal of positioning Europe as the first continent worldwide to achieve climate neutrality by 2050 [1]. This initiative involves implementing strategies aimed at curbing greenhouse gas emissions into the atmosphere. Among these strategies, reducing the reliance on traditional energy sources to meet building energy demands is crucial, accounting for 40 % of energy consumption in Europe and 36 % of greenhouse gas emissions [2], [3].

It is projected that by 2030, approximately 35 million buildings will undergo renovation, focusing on enhancing building envelopes and harnessing renewable resources [4]. Solar energy theoretically has the potential to satisfy global energy demand [5], although its current contributions to global electricity and thermal energy are relatively modest, at 3.6 % and 0.7 %, respectively [6], [7].

Concerning building heating, solar energy integration employs either active or passive systems [8]. In active systems, mechanical and electrical energy powers pumps and fans to transfer solar radiation-absorbing heat transfer fluids, interacting with the environment to be heated. In contrast, passive systems do not require mechanical or electrical components to maintain comfortable conditions using solar energy [9].

Passive heating systems are categorized into isolated gain, direct gain, and indirect gain systems. Isolated gain systems capture solar radiation through a system isolated from the environment to be heated. Direct gain systems allow solar radiation to enter indoor spaces directly through transparent surfaces, where it is absorbed by capacitive masses within the environment, releasing accumulated thermal energy during

nighttime to maintain comfort conditions. Conversely, indirect gain systems accumulate solar radiation in high thermal capacity walls for delayed release into heated environments [10].

The Trombe wall belongs to the category of indirect gain passive systems, comprising a structural building wall (typically the south-facing wall in the northern hemisphere) with high thermal capacity, adjacent to a glazed surface that creates an air gap known as the solar space [11].

Trombe wall can be ventilated or non-ventilated, depending on the presence of two vents, one upper and one lower, created on the high thermal capacity wall [12]. Non-ventilated Trombe wall absorbs incident solar radiation and, subsequently, this accumulated thermal energy is transferred by conduction along the massive wall, for then being partially exchanged by radiation with other surfaces and partially released by convection to the air present inside the adjacent wall [13]. Ventilated Trombe wall also exploits the buoyancy forces generated as a result of the contact between the air inside the solar space and the warm massive wall to heat the indoor environment. Specifically, the air inside the environment enters the solar space through the lower vent, receives heat by convection, and is released warmer through the upper vent [14]. To avoid the risk of overheating during the summer period, fixed and/or movable shading devices are provided. Additionally, the installation of controlled openings on the glazed surface allows for the exploitation of the chimney effect to ventilate the indoor environment [15].

Over the years, several variants of the conventional Trombe wall have been proposed. At the NREL Visitor Centre, a prototype of zigzag Trombe wall has been built, consisting of a southeast-facing glazed wall (to provide light and heat in the morning) and two classical Trombe walls arranged in a V shape, to accumulate heat during the day and release it at night [16]. Water wall uses water as storage material instead of masonry, aiming to reduce radiative losses to the exterior, given that the water surface reaches lower temperatures compared to those achieved by masonry [17]. To improve summer performance, a hybrid Trombe wall prototype has been proposed in which porous ceramics able to absorb water injected through nozzles are inserted. The evaporation of water removes heat from the solar space through the phenomenon of evaporative cooling [18]. Trombe wall with phase change materials (PCMs) exploits the high latent heat of fusion of these materials to increase storage capacity without excessively overloading the structure [19]. Composite Trombe wall consists of an external glass, a non-ventilated solar space, a massive wall without vents, an air gap and an insulated wall with vents. Energy is mainly transferred to the heated environment through natural ventilation, with only a small fraction being transmitted by conduction from the insulated wall to the indoor environment. This configuration helps reduce heat losses during the heating period and undesired heat gains during the cooling period [20]. fluidized Trombe wall contains highly absorbent and low-density material particles within the solar space. Fluidized beds provide heat exchange coefficients an order of magnitude higher than single-phase airflow. Air is circulated within the solar space by fans and absorbs heat from the fluidized particles. Filters are used to avoid transport of particles by air into the environment [21]. Photovoltaic Trombe wall is characterized by photovoltaic modules on the glass surface, in the solar space or on the surface of the massive wall. The air circulating in the solar space heats up and removes heat from the photovoltaic module, increasing its efficiency in electricity production. Additionally, the colours of the photovoltaic modules enhance the aesthetic appearance of the Trombe wall [22]. Further performance enhancement can be achieved by applying selective coatings onto the massive wall, characterized by high values of solar radiation absorption coefficient at short wavelengths and low values of emissivity coefficient at high wavelengths [23]. Regarding the glazed surface, the main influencing parameters are thickness, type and number of glass layers, as they determine convective and radiative heat losses to the outside [24], [25]. Zalewski et al. [26] proposed a numerical model, validated by an extensive experimental campaign, showing how the use of low-emissivity double glazing compared to a single standard glass significantly increases the thermal energy subsequently transferred to the indoor environment. It is also evident that this increase depends on the type of Trombe wall and the location considered. Briga-Sá et al. [27] verified the performance dependence on the thickness of the massive wall, achieving a maximum savings on the thermal requirement of 16.36 %. Askari et al. [28] found that the best energy performance of the Trombe wall is achieved for a solar space depth of 0.2 m, resulting in a reduction in winter energy consumption of 34 %. Chen et al. [29] proposed a wavy-shape Trombe wall that improves airflow and air temperature inside the solar space, resulting in a 68 % higher thermal flux than that obtained with the conventional Trombe wall. Rabani et al. [30] conducted an experimental study on a Trombe wall installed on one half of the south wall of a test chamber in Iran. The wall has three vertical glazed surfaces, one facing south, one east, and one west, to capture solar radiation from sunrise to sunset. Experimental results show that the maximum hourly stored energy occurs in February, amounting to 5800 kJ/h, while during the winter period, the indoor environment temperature remains between 15 °C and 30 °C. Simoes et al. [31] dynamically simulated the behaviour of a Trombe wall to assess the effectiveness of various solutions to reduce the risk of overheating during the summer period. A parametric analysis was conducted to evaluate the effect of solar space depth and vents size on passive ventilation system performance, and it was found that variations in both parameters between 5 and 30 cm slightly influence the results. Night-time ventilation and the presence of fixed and mobile shading devices help limit the increase in energy consumption for cooling during the summer period. In the winter period, a 20 % reduction in thermal requirement is observed.

In this article, a dynamic analysis of the winter energy performance of two Trombe walls installed on the south-facing wall of the test station of the University of Calabria (Rende) has been conducted. For this purpose, DesignBuilder software was used. No article includes a parametric analysis varying all construction parameters such as: the material constituting the support structure of the Trombe walls, the type and number of glass layers, the depth of the solar space and the size of the vents. This parametric study is essential to evaluate the influence on Trombe wall performance in terms of reducing thermal requirements during the winter period.

In Section 2, geometric and thermophysical parameters of the building and the proposed passive system, the assumed operational conditions, and the climatic data used are provided. Finally, the methodology employed to identify the optimal configuration through various dynamic simulations is described. Section 3 presents the results obtained from the simulations, while Section 4 critically discusses these results considering the relationship between key construction parameters, operational conditions, climatic data, and the performance of the passive system. Lastly, Section 5 summarizes the main findings, suggests

potential applications for the proposed system, and outlines future developments of this work.

2. METHODOLOGY

This study assesses the reduction in heating thermal requirements achieved by installing two Trombe walls adjacent to the window on the southern wall of the variable orientation test chamber at the University of Calabria (Rende, Italy). Additionally, it evaluates how this reduction depends on the main construction parameters of the Trombe walls.

The internal dimensions of the heated volume are $4 \times 4 \times 3.2$ m³. The building comprises a single chamber defined by three insulated vertical walls, the designated test vertical wall for the installation of the Trombe walls adjacent to the window, and a floor and ceiling. The glazed system, measuring 1.2×1.5 m², features an aluminium frame with a thermal break and double glazing 4/12air.

The assumption of a grey body with an emissivity coefficient (ε) equal to the absorption coefficient (α) was made for the insulated vertical walls and the test wall. Different values of these coefficients were used for the two wall types, 0.3 for the test wall and 0.6 for the insulated vertical walls [32], to account for the different applied coatings, see Figure 1.

The test station includes an entrance door on the west-facing insulated wall with an area of 1.9 m² and a steady-state thermal transmittance of 2.5 W/(m² K). Table 1, Table 2, Table 3, and Table 4 detail the composition of all building components, layer thicknesses, thermal conductivities, and the corresponding conductive thermal resistances. Table 5 lists internal and external thermal conductances, thermal resistances and the steady-state thermal transmittances of each opaque and transparent building component. Hourly thermal requirements for heating were calculated using the DesignBuilder dynamic simulation software. To enable performance comparison, simulations were conducted for both the reference building and the building improved with two Trombe walls. The software identified the location by entering a latitude of 39° 18', while climatic data on direct and diffused solar radiation, temperature, humidity, and air velocity were extrapolated from the National IGDG Database (Italian Climatic data collection "Gianni De Giorgio").

The test chamber was modelled in three dimensions using the previously described layers. Additionally, the following conditions were imposed:

- Office as the intended use;
- Absence of occupants;
- Absence of artificial lighting;
- Infiltration of external air considered in the calculation through a 5 % opening of the awning window;
- Natural gas heating system exclusively for maintaining indoor air temperature at the setpoint value of 20 °C;
- On weekdays, the heating system operates at full load from 05:00 a.m. to 07:00 p.m., turned off during the night and on holidays.

The initial dynamic simulation aimed to determine the current thermal requirements of the test chamber. Subsequently, passive components were integrated to evaluate the associated reduction in energy consumption. The Trombe walls were modelled as two distinct cavities without inputs from heating systems, artificial lighting, or occupants. Each solar space was horizontally bounded by PVC extensions of the ceiling and floor, and vertically by a single 4 mm thick glass (Sgl Clr 4mm) facing south,

Figure 1. Variable orientation test station.

with two vertical PVC walls, see Figure 2. The resulting solar space measures 0.32 m in depth and 1.71 m in width. The wall separating the solar space from the indoor environment was coated with dark paint, having absorption and emission coefficients of 0.9, while the external test wall maintained coefficients of 0.3 between the Trombe walls.

On each massive absorbing wall, two vents were modelled: one lower for air intake from the indoor environment and one upper for releasing heated air into the environment. The vents, symmetrically positioned relative to the transmission surface with the indoor environment, measured 1.0 m in width and 0.5 m in height, and remained open from 8:00 a.m. to 6:00 p.m. Following the Trombe wall modelling, a second dynamic simulation was conducted to compute the new winter thermal requirement.

To identify an optimal configuration for reducing heating thermal requirements, various dynamic simulations were performed, varying the main construction parameters of the Trombe walls, see Table 6.

Initially, the support structure material was varied, comparing the consumption impact of aluminium versus PVC. While a slight consumption improvement was noted with aluminium, the cost difference did not justify its application. Subsequently, the influence of the type of vertical glazed surface was evaluated. The single Sng Clr 4mm glass was replaced with standard Dbl Clr 4/12air and low-emissivity Dbl LoE Clr 3/13air glass ($\varepsilon = 0.2$), showing significant improvement with the latter.

Continuing with low-emissivity double glass, simulations were conducted using three glazed surfaces to increase solar radiation transmission, see Figure 3. Glazed surfaces facing west and east were also of Dbl LoE Clr 3/13air glass, supported by a PVC structure. Results indicated substantial reductions in heating thermal requirements compared to configurations with only south-facing glazed surfaces.

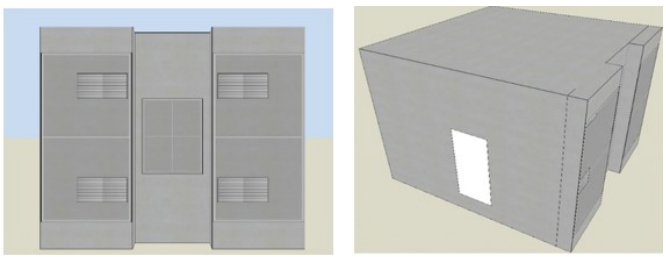

Figure 2. Three-dimensional model of the building equipped with two Trombe walls.

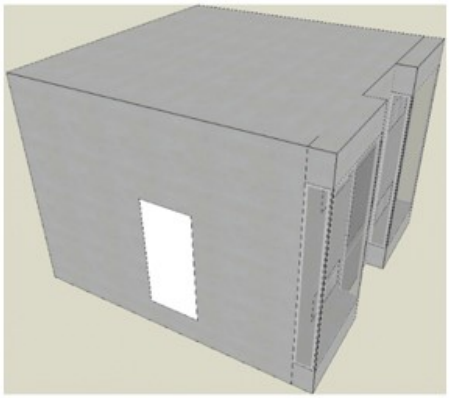

Figure 3. Vertical glazed surfaces on the west, south and east exposures of the solar spaces.

The study then varied the vent cross-sectional area, fixing the nominal width at 1.0 m while varying the height from 0.1 m to 0.6 m in increments of 0.1 m. Similarly, with a fixed height of 0.5 m, the width ranged from 0.4 m to 1 m in increments of 0.1 m.

Results showed that winter thermal requirements increased with larger cross-sectional areas, mainly influenced by total area rather than individual dimensions. Comparing to a nominal cross-sectional area of 0.5 m², the smallest area evaluated was 0.1 m², derived from a width of 1 m and height of 0.1 m. These dimensions were chosen for a parametric analysis varying solar space depth.

Compared to the nominal 0.32 m, reduced thermal requirements were observed at depths of 0.1 m and 0.2 m, with an increase at 0.4 m; the maximum reduction occurred at 0.2 m.

Ultimately, the optimal configuration for reducing heating thermal requirements featured a solar space depth of 0.20 m, supported by a PVC structure with three glazed surfaces of low-emissivity double glass and a 13 mm air gap. This setup included two vents, each with an area of 0.1 m², ensuring natural air circulation, see Table 6.

3. RESULTS

Referring to Table 6, this section details the findings from dynamic simulations performed with DesignBuilder, focusing on the primary energy consumption of the heating system. Simulations were conducted on an hourly basis, and to facilitate comparison between different Trombe wall setups, the results were aggregated monthly and standardized to the net floor area of the test chamber, which is 16 m². Upon determining the optimal configuration, a more detailed analysis was provided by

Table 1. Stratigraphy of insulated vertical walls.

Layer	Material	*t* (m)	*ρ* (kg/m³)	*c* (J/(kg·K))	*λ* (W/(m·K))	*R* (m²·K/W)
1	Plaster	0.02	1800	910	0.900	0.022
2	Perforated brick	0.08	1000	840	0.360	0.222
3	Insulator (Styrodur)	0.30	15	1220	0.035	8.571
4	Perforated brick	0.08	1000	840	0.360	0.222
5	Electrowelded mesh	0.0005	7870	1990	80.000	0.000006
6	Plaster	0.02	1800	910	0.900	0.022

Table 2. Stratigraphy of test wall and double-glazed window.

Layer	Material	*t* (m)	*ρ* (kg/m³)	*c* (J/(kg·K))	*λ* (W/(m·K))	*R* (m²·K/W)
1	Plaster	0.015	1800	910	0.900	0.017
2	Brick (RDB)	0.30	650	840	0.231	1.299
3	Plaster	0.015	1800	910	0.900	0.017
4	Glass	0.40	2000	830	0.900	0.004
5	Air gap	0.12	1.200	1000	0.035	0.034
6	Glass	0.40	2000-	830	0.900	0.004

Table 3. Stratigraphy of floor.

Layer	Material	*t* (m)	*ρ* (kg/m³)	*c* (J/(kg·K))	*λ* (W/(m·K))	*R* (m²·K/W)
1	Tiles	0.01	2300	840	1.000	0.010
2	Slc with expanded clay	0.15	1200	800	0.160	0.938
3	Insulator (Styrodur)	0.30	15	1220	0.035	8.571
4	Concrete	0.05	2300	1000	1.160	0.043

Table 4. Stratigraphy of ceiling.

Layer	Material	*t* (m)	*ρ* (kg/m³)	*c* (J/(kg·K))	*λ* (W/(m·K))	*R* (m²·K/W)
1	Plaster	0.02	1800	910	0.900	0.022
2	Hollow-core concrete slab	0.16	1700	850	0.900	0.178
3	Insulator (Styrodur)	0.30	15	1220	0.035	8.571
4	Eaves gutter	0.0008	2700	900	52.000	0.00002

Table 5. Internal and external conductances, thermal resistances and steady-state thermal transmittance of building components.

Component	h_i (W/(m² K))	h_e (W/(m² K))	R_i (m² K/W)	R_e (m² K/W)	U (W/ (m² K))
Insulated vertical wall	8.15	25.00	0.123	0.040	0.108
Test wall	7.7	25.00	0.130	0.040	0.667
Floor	7.7	25.00	0.130	0.040	0.103
Ceiling	7.7	25.00	0.130	0.040	0.112
Door	-	-	-	-	2.500
Double-glazed window	7.7	25.00	0.130	0.040	4.690

Table 6. Analysed configurations.

Configuration [-]	Supporting material [-]	Type of glazing [-]	Number of glazings [-]	Vents cross-sectional area (m²)	Solar space depth (m)
0	-	-	-	-	-
1	PVC	Sng Clr 4mm	1	0.50	0.32
2	Aluminum	Sng Clr 4mm	1	0.50	0.32
3.1	PVC	Dbl Clr 4/12$_{air}$	1	0.50	0.32
3.2		Dbl LoE Clr 3/13$_{air}$	1	0.50	0.32
4	PVC	Dbl LoE Clr 3/13$_{air}$	3	0.50	0.32
5.1	PVC	Dbl LoE Clr 3/13$_{air}$	3	0.10	0.32
5.2				0.20	0.32
5.3				0.25	0.32
5.4				0.30	0.32
5.5				0.35	0.32
5.6				0.40	0.32
5.7				0.45	0.32
5.8				0.60	0.32
6.1	PVC	Dbl LoE Clr 3/13$_{air}$	3	0.10	0.10
6.2					0.20
6.3					0.40
Optimal	**PVC**	**Dbl LoE Clr 3/13$_{air}$**	**3**	**0.10**	**0.20**

presenting the thermal requirements on an hourly basis for each month. Furthermore, the average temperature of the heated space was illustrated.

Figure 4 displays the monthly heating thermal requirements for the test station in its baseline state (configuration 0) and with the two Trombe walls in the standard setup (configuration 1). Figure 5 presents a comparison of monthly thermal requirements based on the material of the support structure for the glazed surface (aluminium versus PVC). Figure 6 depicts the monthly fluctuations in heating thermal requirements concerning the type of glazed surface, including single glass, double glass, and double low-emissivity glass. In Figure 7, the comparison of heating energy consumption is illustrated based on the number of vertical glazed surfaces enclosing the solar space. Configuration 3.2 features a single vertical glazed surface oriented south, with

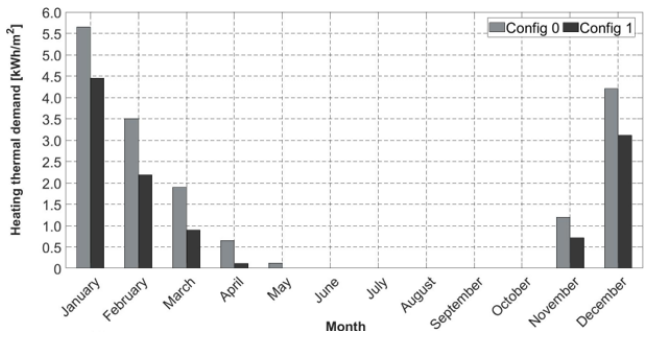

Figure 4. Monthly heating thermal demand of the test station without Trombe walls and with Trombe walls in the standard configuration.

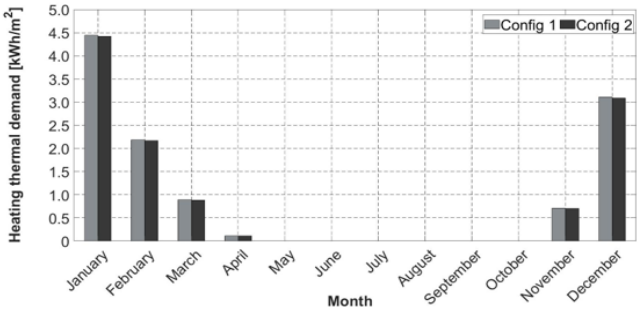

Figure 5. Monthly heating thermal demand as a function of the support structure of the Trombe walls.

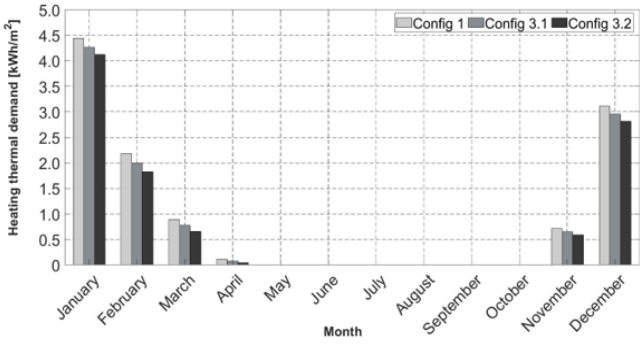

Figure 6. Monthly heating thermal demand varying with the type of glazed surface.

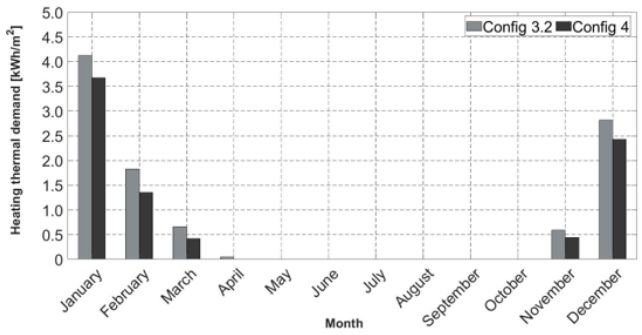

Figure 7. Monthly heating thermal demand varying with the number of glazed surfaces defining the solar space.

the east and west vertical surfaces made of PVC panels. Conversely, in Configuration 4, the solar space is enclosed by vertical glazed surfaces consisting of low-emissivity double glazing on all three sides.

Figure 8 depicts the winter thermal demands based on the cross-sectional area of the vents. For consistency in the representation of results, the requirements for areas of 0.15 m² and 0.55 m² were derived through linear interpolation. The results were aggregated annually to facilitate a clear comparison of consumption differences between configurations, as monthly variations are minimal. Figure 9 illustrates how monthly thermal requirements vary with the depth of the solar space.

For the optimal configuration 6.2, the hourly heating thermal demands for each winter month are depicted in Figure 10, Figure 11, Figure 12, Figure 13, and Figure 14. For each month of the heating season, the trends in thermal demand and average indoor temperature on an hourly basis for two characteristic days are presented. The period from January 6th to 7th was chosen as it represents the system's behaviour after a heating plant shutdown phase, see Figure 10 and Figure 15.

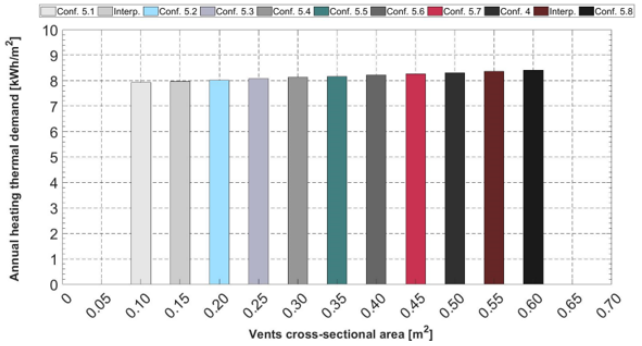

Figure 8. Annual heating thermal demand varying with the cross-sectional area of the vents.

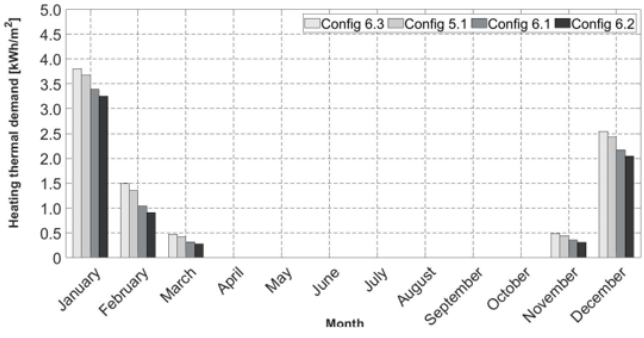

Figure 9. Monthly heating thermal demand varying with the depth of the solar space.

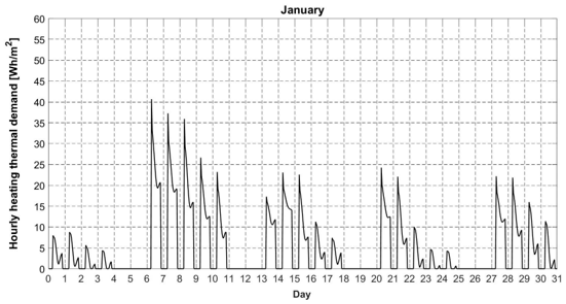

Figure 10. Hourly heating thermal demand for the month of January.

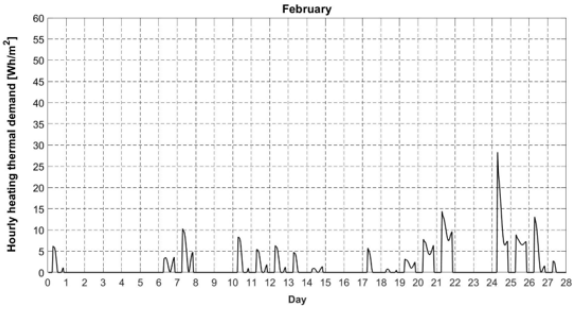

Figure 11. Hourly heating thermal demand for the month of February.

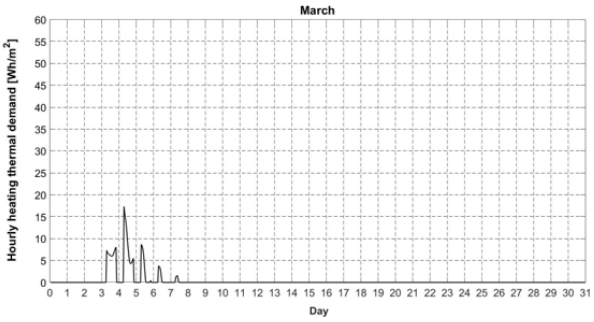

Figure 12. Hourly heating thermal demand for the month of March.

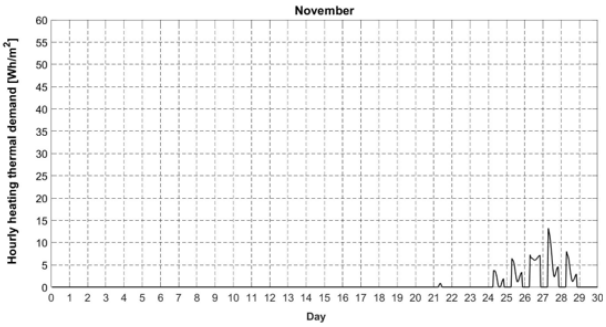

Figure 13. Hourly heating thermal demand for the month of November.

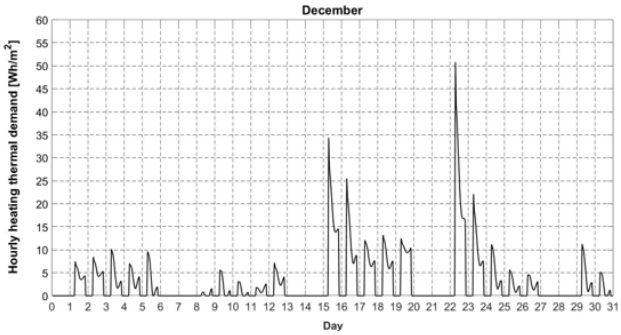

Figure 14. Hourly heating thermal demand for the month of December.

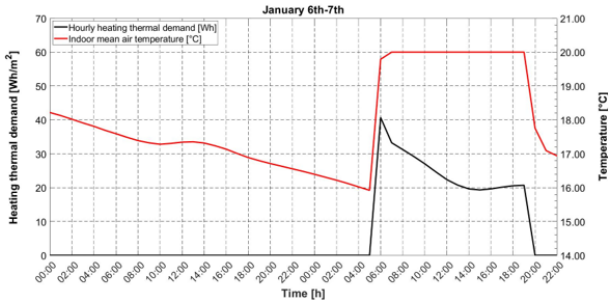

Figure 15. Hourly trend of the heating thermal demand and the average temperature from January 6th to 7th.

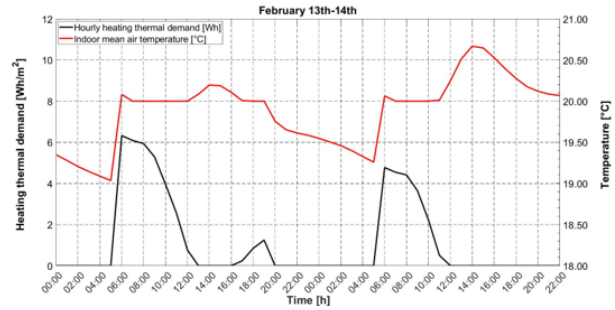

Figure 16. Hourly trend of the heating thermal demand and the average temperature from February 13th to 14th.

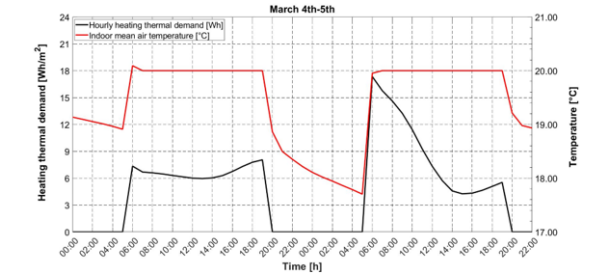

Figure 17. Hourly trend of the heating thermal demand and the average temperature from March 4th to 5th.

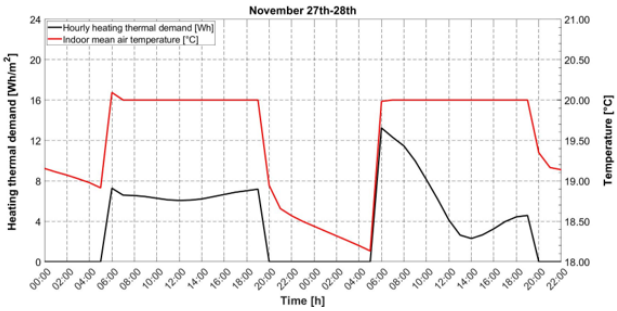

Figure 18. Hourly trend of the heating thermal demand and the average temperature from November 27th to 28th.

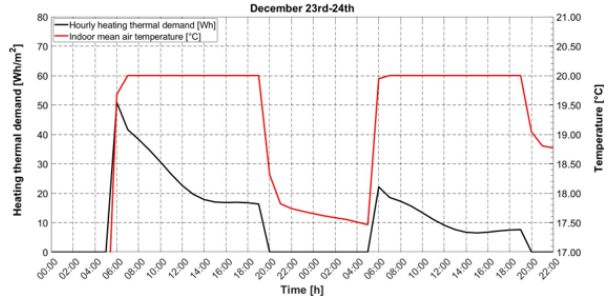

Figure 19. Hourly trend of the heating thermal demand and the average temperature from December 23rd to 24th.

Figure 16 illustrates the trends for two days in mid-February. In reference to Figure 12 and Figure 13, the two days in the middle of the operational period of the heating system are highlighted in Figure 17 and Figure 18. Lastly, Figure 19 shows the period from December 23rd to 24th, featuring the peak hourly winter thermal demand, which reaches 50.79 W h/m².

4. DISCUSSION

The current winter energy demand per unit area of the test structure stands at 17.23 kW h/m². Upon implementation of Trombe walls in the standard layout, this requirement drops to 11.47 kW h/m², marking a 33.43 % decrease. As depicted in Figure 5, utilizing aluminum for the support structure results in a marginal 0.77 % reduction in energy consumption compared to the standard configuration. Given this slight improvement and the cost differential between aluminum and PVC, the parametric analysis proceeded with PVC support structures.

Conversely, Figure 6 illustrates significant enhancements in monthly thermal requirements when employing both double glazing and low-emissivity double glazing, achieving reductions compared to the standard setup of 6.51 % and 12.30 %, respectively. The benefit derived from low-emissivity double glazing over simple double-glazing amounts to 6.20 %. This improvement is attributed to the reduction of convective losses to the external environment by the air gap in double glazing, while low-emissivity double glazing further mitigates radiative losses at longer wavelengths.

Figure 7 demonstrates that Trombe walls featuring low-emissivity vertical glazed surfaces on both east and west exposures lead to decreased monthly thermal demands due to enhanced solar radiation absorption in the solar spaces. Specifically, total consumption during winter is reduced by 17.33 % compared to surfaces with low-emissivity glazing only on the main south exposure. Moreover, in this configuration, the passive solar system completely offsets the heating load in April.

Figure 8 emphasizes the direct correlation between annual winter thermal demand and vent area. Reducing the vent size from 0.5 m² to 0.1 m² results in a 4.53 % decrease in total winter consumption. This improvement stems from reduced air flow rate due to increased pressure drop associated with the smaller cross-sectional area. Consequently, under similar solar radiation conditions, a lower air flow rate results in higher enthalpy content, offsetting the adverse impact of introducing less heated air into the environment.

Figure 9 illustrates that an optimal solar space depth of 0.20 m (configuration 6.2) reduces winter thermal demands by 14.52 % compared to the nominal depth of 0.32 m (configuration 5.1). This behavior mirrors that of vent size optimization. However, further reducing the passage area to 0.10 m (configuration 6.1) increases winter consumption, indicating that insufficient heated air introduction outweighs any benefits from narrower solar spaces.

Configuration 6.2 emerges as the optimal solution, with a winter thermal requirement of 6.79 kW h/m², corresponding to a 60.62 % reduction compared to the test station's winter thermal demand without Trombe walls integration. For this configuration, it is evident that in March the thermal energy demand is present only at the beginning of the month; subsequently, the passive system completely compensates the winter heating load. Similarly, in November, the heating system only operates during the last few days of the month. On January 6th, despite the heating system being off, due to convective,

radiative, and natural ventilation phenomena typical of the Trombe walls, the average indoor temperature decreases following a mitigated free evolution. Between 12:00 and 13:00, due to the peak solar radiation, the temperature rises to 17.35 °C and then decreases to 15.92 °C. On January 7th, during the activation phase of the heating system, a peak of 40.66 Wh/m² is observed, necessary to restore the temperature in free evolution back to the 20 °C set-point. Subsequently, despite the ambient temperature remaining at 20 °C, the thermal demand decreases due to the Trombe walls. From 15:00 to 19:00, the thermal requirement increases due to the absence of solar radiation. However, this increase is limited by the release of accumulated thermal energy within the Trombe walls. On February 13th, it can be observed that even during the night-time heating system shutdown phase, the temperature remains above 19 °C. Again, a thermal requirement peak is recorded during the heating system activation, but this time the requirement decreases to zero during the solar radiation peak, with an increase in the average room temperature to 20.19 °C. Between 16:00 and 19:00, the thermal requirement slightly increases and subsequently, when the system is turned off, the temperature decreases until 05:00 on February 14th. At this point, the heating system is turned back on to restore the temperature from 19.26 °C back up to 20 °C. Once again, the thermal demand drops to zero at 12:00 and the average room temperature reaches 20.67 °C at 14:00. However, in this scenario, the thermal energy released by the Trombe walls manages to offset the heating load for the rest of the day. On December 23rd, due to the system being off in the two previous days, the maximum winter period thermal requirement is observed, equal to 50.79 W h/m², necessary to raise the room temperature from 15.13 °C to the set-point value. Subsequently, the thermal demand rapidly decreases until 15:00 and stabilizes at nearly constant values until 19:00. During the night, the temperature drops and reaches 17.46 °C by 05:00 on December 24th. At this point, the heating system turns on, restoring the temperature to 20 °C and a consumption trend similar to that of the previous day is observed, but with lower values, since starting from a higher initial temperature condition.

5. CONCLUSIONS

This article presents a dynamic analysis of the energy performance of two Trombe walls installed on the south-facing wall of the University of Calabria's test station in Rende, Italy. Utilizing DesignBuilder dynamic simulation software, the study aimed to determine the most effective configuration of Trombe walls by varying key construction parameters.

The findings indicate that the winter energy efficiency is minimally impacted by the material used for the support structure of the glazed surface and the size of the vents. In contrast, a significant correlation exists between energy savings and the type and quantity of glazed surfaces defining the solar space. Similarly, the depth of the solar space plays a crucial role in the passive system's energy performance.

Through this parametric study, the optimal configuration reduces heating energy demand by 60.62 % compared to the current setup without Trombe walls. Furthermore, the presence of Trombe walls enhances thermal inertia within the building, resulting in gradual cooling even after the heating system is deactivated. This cost-effective and straightforward solution holds promise for retrofitting existing buildings.

Future research will expand on these findings with Computational Fluid Dynamics (CFD) analysis of the identified optimal configuration. This analysis will assess local velocity and temperature distributions within the solar space and the heated environment, providing deeper insights into the system's performance behaviour.

ACKNOWLEDGEMENT

This work was co-funded by the Next Generation EU - Italian PNRR, Mission 4, Component 2, Investment 1.5, call for the creation and strengthening of 'Innovation Ecosystems', building 'Territorial R&D Leaders' (Directorial Decree n. 2021/3277) - project Tech4You "Technologies for climate change adaptation and quality of life improvement", n. ECS0000009, CUP H23C22000370006.

REFERENCES

[1] S. Wolf, J. Teitge, J. Mielke, F. Schütze, C. Jaeger, The European Green Deal - More Than Climate Neutrality, Intereconomics, vol. 56, no. 2, pp. 99–107, Mar. 2021. DOI: 10.1007/s10272-021-0963-z

[2] C. Fetting, The European Green Deal, ESDN Report, Dec. 2020, ESDN Office, Vienna.

[3] European Commission, Energy efficiency in buildings, Feb. 17, 2020.

[4] European Commission, Renovation Wave: doubling the renovation rate to cut emissions, boost recovery and reduce energy poverty, Oct. 14, 2020.

[5] E. Kabir, P. Kumar, S. Kumar, A. A. Adelodun, K.-H. Kim, Solar energy: Potential and future prospects, Renewable and Sustainable Energy Reviews, vol. 82, Feb. 2018, pp. 894–900. DOI: 10.1016/j.rser.2017.09.094

[6] IEA Renewables, Analysis and forecast to 2025, 2020.

[7] H. H. Pourasl, R. V. Barenji, V. M. Khojastehnezhad, Solar energy status in the world: A comprehensive review, Energy Reports, vol. 10, Nov. 2023, pp. 3474–3493. DOI: 10.1016/j.egyr.2023.10.022

[8] P. A. Østergaard, N. Duic, Y. Noorollahi, H. Mikulcic, S. Kalogirou, Sustainable development using renewable energy technology, Renewable Energy, vol. 146, Feb. 2020, pp. 2430–2437. DOI: 10.1016/j.renene.2019.08.094

[9] H.-Y. Chan, S. B. Riffat, J. Zhu, Review of passive solar heating and cooling technologies, Renewable and Sustainable Energy Reviews, vol. 14, no. 2, Feb. 2010, pp. 781–789. DOI: 10.1016/j.rser.2009.10.030

[10] N. Gupta, G. N. Tiwari, Review of passive heating/cooling systems of buildings, Energy Science & Engineering, vol. 4, no. 5, Oct. 2016, pp. 305–333. DOI: 10.1002/ese3.129

[11] A. K. Nanda, C. K. Panigrahi, A state-of-the-art review of solar passive building system for heating or cooling purpose, Front. Energy, vol. 10, no. 3, Sep. 2016, pp. 347–354. DOI: 10.1007/s11708-016-0403-0

[12] L. Licholai, A. Starakiewicz, J. Krasoń, P. Miąsik, The Influence of Glazing on the Functioning of a Trombe Wall Containing a Phase Change Material, Energies, vol. 14, no. 17, Aug. 2021, p. 5243. DOI: 10.3390/en14175243

[13] G. Gan, 'Simulation of buoyancy-induced flow in open cavities for natural ventilation', Energy and Buildings, vol. 38, May 2006, no. 5, pp. 410–420. DOI: 10.1016/j.enbuild.2005.08.002

[14] R. O. Warrington, T. A. Ameel, Experimental Studies of Natural Convection in Partitioned Enclosures With a Trombe Wall Geometry, Journal of Solar Energy Engineering, vol. 117, no. 1,

Feb. 1995, pp. 16–21.
DOI: 10.1115/1.2847709
[15] F. Stazi, A. Mastrucci, C. Di Perna, The behaviour of solar walls in residential buildings with different insulation levels: An experimental and numerical study, Energy and Buildings, vol. 47, Apr. 2012, pp. 217–229.
DOI: 10.1016/j.enbuild.2011.11.039
[16] O. Saadatian, K. Sopian, C. H. Lim, N. Asim, M. Y. Sulaiman, Trombe walls: A review of opportunities and challenges in research and development, Renewable and Sustainable Energy Reviews, vol. 16, no. 8, Oct. 2012, pp. 6340–6351.
DOI: 10.1016/j.rser.2012.06.032
[17] Y. W. Liu, W. Feng, Integrating Passive Cooling and Solar Techniques into the Existing Building in South China, AMR, vol. 368–373, Oct. 2011, pp. 3717–3720.
DOI: 10.4028/www.scientific.net/AMR.368-373.3717
[18] S. Melero-Tur, I. Morgado-Baca, F. J. Neila-González, C. Acha-Román, Passive Evaporative Cooling by porous ceramic elements integrated in a trombe wall, PLEA 2011 - 27th Conf. on Passive and Low Energy Architecture, Louvain-la-Neuve, Belgium, 13-15 July, 2011.
DOI: 10.5281/zenodo.10557600
[19] L. Zalewski, A. Joulin, S. Lassue, Y. Dutil, D. Rousse, Experimental study of small-scale solar wall integrating phase change material, Solar Energy, vol. 86, no. 1, Jan. 2012, pp. 208–219.
DOI: 10.1016/j.solener.2011.09.026
[20] K. Sergei, C. Shen, Y. Jiang, A review of the current work potential of a trombe wall, Renewable and Sustainable Energy Reviews, vol. 130, Sep. 2020, p. 109947.
DOI: 10.1016/j.rser.2020.109947
[21] M. Tunç, M. Uysal, Passive solar heating of buildings using a fluidized bed plus Trombe wall system, Applied Energy, vol. 38, no. 3, Jan. 1991, pp. 199–213.
DOI: 10.1016/0306-2619(91)90033-T
[22] W. Sun, J. Ji, C. Luo, W. He, Performance of PV-Trombe wall in winter correlated with south façade design, Applied Energy, vol. 88, no. 1, Jan. 2011, pp. 224–231.
DOI: 10.1016/j.apenergy.2010.06.002
[23] N. P. Nwachukwu, W. I. Okonkwo, Effect of an Absorptive Coating on Solar Energy Storage in a Thrombe wall system, Energy and Buildings, vol. 40, 2008, no. 3, pp. 371–374.
DOI: 10.1016/j.enbuild.2007.03.004
[24] O. Saadatian, K. Sopian, C. H. Lim, N. Asim, M. Y. Sulaiman, Trombe walls: A review of opportunities and challenges in research and development, Renewable and Sustainable Energy Reviews, vol. 16, Oct. 2012, no. 8, pp. 6340–6351.
DOI: 10.1016/j.rser.2012.06.032
[25] Z. Hu, W. He, J. Ji, S. Zhang, A review on the application of Trombe wall system in buildings, Renewable and Sustainable Energy Reviews, vol. 70, Apr. 2017, pp. 976–987.
DOI: 10.1016/j.rser.2016.12.003
[26] L. Zalewski, S. Lassue, B. Duthoit, M. Butez, Study of solar walls — validating a simulation model, Building and Environment, vol. 37, Jan. 2002, no. 1, pp. 109–121.
DOI: 10.1016/S0360-1323(00)00072-X
[27] A. Briga-Sá, A. Martins, J. Boaventura-Cunha, J. C. Lanzinha, A. Paiva, Energy performance of Trombe walls: Adaptation of ISO 13790:2008(E) to the Portuguese reality, Energy and Buildings, vol. 74, May 2014, pp. 111–119.
DOI: 10.1016/j.enbuild.2014.01.040
[28] M. Askari, M. H. Jahangir, Evaluation of thermal performance and energy efficiency of a Trombe wall improved with dual phase change materials, Energy, vol. 284, Dec. 2023, p. 128587.
DOI: 10.1016/j.energy.2023.128587
[29] H. Chen, S. Liu, M. Eftekhari, Y. Li, W. Ji, Y. Shen, Experimental studies on the energy performance of a novel wavy-shape Trombe wall, Journal of Building Engineering, vol. 61, Dec. 2022, p. 105242.
DOI: 10.1016/j.jobe.2022.105242
[30] M. Rabani, V. Kalantar, A. A. Dehghan, A. K. Faghih, Experimental study of the heating performance of a Trombe wall with a new design, Solar Energy, vol. 118, Aug. 2015, pp. 359–374.
DOI: 10.1016/j.solener.2015.06.002
[31] N. Simões, M. Manaia, I. Simões, Energy performance of solar and Trombe walls in Mediterranean climates, Energy, vol. 234, Nov. 2021, p. 121197.
DOI: 10.1016/j.energy.2021.121197
[32] S. Fantucci, V. Serra, Experimental Assessment of the Effects of Low-Emissivity Paints as Interior Radiation Control Coatings, Applied Sciences, vol. 10, Jan. 2020, no. 3, p. 842.
DOI: 10.3390/app10030842